A Letters Journal Exploring
the Frontiers of Physics

OFFPRINT

Coupling of actin hydrolysis and polymerization: Reduced description with two nucleotide states

X. Li, R. Lipowsky and J. Kierfeld

EPL, **89** (2010) 38010

Please visit the new website
`www.epljournal.org`

TARGET YOUR RESEARCH WITH EPL

Sign up to receive the free EPL table of contents alert.

www.epljournal.org/alerts

epl A Letters Journal Exploring the Frontiers of Physics

February 2010

EPL, **89** (2010) 38010 www.epljournal.org
doi: 10.1209/0295-5075/89/38010

Coupling of actin hydrolysis and polymerization: Reduced description with two nucleotide states

X. Li[1,2], R. Lipowsky[1] and J. Kierfeld[3(a)]

[1] *Max Planck Institute of Colloids and Interfaces - Science Park Golm, 14424 Potsdam, Germany, EU*
[2] *Key Laboratory of Frontiers in Theoretical Physics, ITP, CAS - Beijing 100090, China*
[3] *Physics Department, TU Dortmund University - 44221 Dortmund, Germany, EU*

received 1 July 2009; accepted in final form 19 January 2010
published online 22 February 2010

PACS 87.16.Ka – Filaments, microtubules, their networks, and supramolecular assemblies
PACS 87.16.A- – Theory, modeling, and simulations
PACS 87.15.rp – Polymerization

Abstract – The polymerization of actin filaments is coupled to the hydrolysis of adenosine triphosphate (ATP), which involves both the cleavage of ATP and the release of inorganic phosphate. We describe hydrolysis by a reduced two-state model with a cooperative cleavage mechanism, where the cleavage rate depends on the state of the neighboring actin protomer in a filament. We obtain theoretical predictions of experimentally accessible steady-state quantities such as the size of the ATP-actin cap, the size distribution of ATP-actin islands, and the cleavage flux for cooperative cleavage mechanisms.

Copyright © EPLA, 2010

Introduction. – Actin filaments are an important structural element of the cytoskeleton, and their ATP-driven polymerization dynamics plays an important role in cell motility [1]. The ATP-hydrolysis in actin filaments is the basis for treadmilling, *i.e.*, the simultaneous polymerization and depolymerization at the two ends of a filament, and is necessary for actin-mediated force generation and motility [2].

Actin monomers (G-actin) assemble into polar actin filaments (F-actin) with a fast polymerization dynamics at the barbed end and a slow polymerization dynamics at the pointed end. Actin monomers can bind ATP, which is then hydrolyzed in a two-step process into adenosine diphosphate (ADP) and inorganic phosphate ($\mathrm{P_i}$). First, ATP is cleaved into the complex ADP-$\mathrm{P_i}$, from which $\mathrm{P_i}$ is released in a second step. After incorporation into a filament the actin protomers can therefore be in three different states: a T-state (ATP-actin), a Θ-state (ADP-$\mathrm{P_i}$-actin), and a D-state (ADP-actin).

Past studies have focused on two sorts of cleavage processes in actin filaments. In *random cleavage*, T-protomers are cleaved independent of the state of their neighbors [3–5]. In *vectorial cleavage*, there is a sharp interface between the ATP-cap containing only T-protomers and the remaining filament consisting of Θ- and D-protomers, and cleavage can only occur at the TΘ-interface [6–9].

In this letter, we investigate *cooperative* hydrolysis mechanisms, where the cleavage rate of each monomer depends on the state of its neighbors and which contain random and vectorial mechanisms as special cases. Cooperative hydrolysis was previously discussed in ref. [10] for actin and ref. [11] for microtubules. One important piece of evidence for a cooperative hydrolysis is the small hydrolysis rate of G-actin as compared to F-actin, which acts as a very effective ATPase with a fast hydrolysis rate. This pronounced change of the ATP-hydrolysis rate after inclusion of G-actin monomers into filaments suggests that the cleavage rate is affected by binding to other protomers in the filament. Furthermore, structural differences between T- and D-state protomers indicate that cleavage might be affected by the same structural elements that are also involved in the binding of protomers [12,13].

A complete model of ATP-hydrolysis involves all three nucleotide states of actin protomers. We have studied such three-state models for cooperative ATP-hydrolysis in ref. [14]. In this letter, we will consider a reduced two-state model by combining the Θ-state and the D-state of protomers into a single D*-state. This means that we focus on the cleavage of T-protomers and ignore the subsequent process of $\mathrm{P_i}$ release. The reduction to two protomer states can be justified for fast growth at

---

[(a)] E-mail: Jan.Kierfeld@tu-dortmund.de

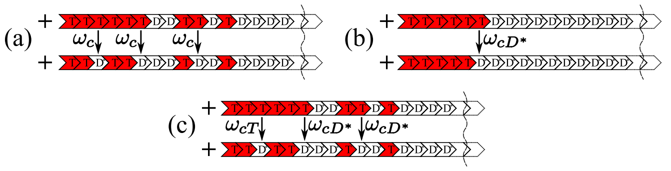

Fig. 1: (Colour on-line) Actin filament consisting of T-protomers (red) and D*-protomers (white) in the reduced two-state model. (a) Random cleavage with rate ω_c; (b) vectorial cleavage with rate ω_{c,D^*}; (c) cooperative cleavage with rate ω_{c,D^*} and $\omega_{c,T}$ depending on the local neighborhood.

high T-monomer concentrations. The reduced model has the advantage that we are able to obtain analytic predictions for important steady-state observables, such as the size of the ATP-actin cap, the size distribution of ATP-actin islands, and the cleavage flux. In particular, we can calculate analytically how these quantities depend on the cooperativity of the cleavage mechanism. We find an intriguing scaling behavior in the limit of strongly cooperative cleavage.

Two-state model for cooperative hydrolysis. – In the reduced two-state model, we combine the Θ-state and the D-state of protomers into a single D*-state and model the actin filament as a one-dimensional sequence of actin monomers in the T- or D*-state (ignoring the helical structure of the filament), see fig. 1.

In general, cleavage within the actin filament happens according to a cooperative mechanism, *i.e.*, the cleavage rate of each monomer depends on the state of its neighbors. Each monomer is *polar*, therefore we do not expect cleavage and release rates to be mirror symmetric, *i.e.*, they need not to be invariant under exchange of the two neighbors. The simplest way to introduce cooperativity without mirror symmetry is to assume that the cleavage rate depends on the state of the neighbor in the direction of one of the ends. Because the ATP-binding cleft is located in the direction of the pointed end, it is plausible to assume that cleavage depends on the state of the neighbor monomer on the "pointed side". Consequently, we introduce two cleavage rates for an ATP-monomer: ω_{cT} if the monomer has a T-neighbor on the pointed side and ω_{cD^*} if the monomer has a D*-neighbor on the pointed side. The two cleavage rates ω_{cT}, ω_{cD^*}, can also be written as

$$\omega_{cD^*} \equiv \omega_c, \qquad \omega_{cT} \equiv \omega_c \rho_c, \tag{1}$$

which defines the *cleavage parameter* ρ_c. We assume that the presence of a cleaved neighbor monomer *increases* the cleavage rate, which implies $\rho_c \leqslant 1$. In the special case of $\rho_c = 1$, the cleavage rate does *not* depend on the state of neighboring monomers, which corresponds to *random* cleavage. In the limiting case of $\rho_c = 0$, cleavage *only* happens at the TD*-interface within the filament corresponding to a *vectorial* cleavage mechanism. A small cleavage parameter $\rho_c \ll 1$ corresponds to a strongly cooperative cleavage mechanism.

Table 1: Literature values for model parameters.

κ_{on} (μM^{-1} s^{-1})	$\omega_{\text{off},T}$ (s^{-1})	ω_{on,D^*}	ω_c (s^{-1})
11.6 [5,15]	1.4 [5,15]	0	0.3 [3]

In the following, we will focus on the barbed end of the filament. T-monomers attach with a rate ω_{on} (the number of T-monomers attaching per unit time) at the barbed end. This attachment rate is proportional to the concentration C_T of T-monomers in solution and the rate constant κ_{on}, *i.e.*, $\omega_{\text{on}} = \kappa_{\text{on}} C_T$. We assume that the attachment of D*-monomers is not possible, *i.e.*, $\omega_{\text{on},D^*} = 0$, which is justified in view of smaller rate constants [5] and small concentrations of Θ- and D-monomers in solution.

Both T- and D*-monomers can detach from the barbed end with rates $\omega_{\text{off},T}$ and ω_{off,D^*}. Starting from the full three-state model, an effective detachment rate ω_{off,D^*} of D*-monomers can only be defined consistently for the whole T-monomer concentration range C_T if Θ- and D-monomers have similar detachment rates, $\omega_{\text{off},\Theta} \simeq \omega_{\text{off},D}$. Measured values $\omega_{\text{off},\Theta} \simeq 0.2\,\text{s}^{-1}$ and $\omega_{\text{off},D} \simeq 5.4\,\text{s}^{-1}$ [5] show that this condition is violated. Nevertheless, a reduced two-state model can still be introduced for high T-monomer concentrations C_T, where the probability P_{1,D^*} that the first protomer at the barbed end is a D*-protomer is negligible or the probability $P_{1,T}$ that the first protomer at the barbed end is a T-protomer is close to one,

$$P_{1,D^*} \approx 0 \quad \text{and} \quad P_{1,T} = 1 - P_{1,D^*} \approx 1. \tag{2}$$

In this limit the corresponding detachment flux of D*-monomers $P_{1,D^*}\omega_{\text{off},D^*} \approx 0$ is always negligible, and the detachment rates of both Θ- and D-monomers become irrelevant for the polymerization process. In the following we will focus on this limit $P_{1,D^*} \approx 0$. We will show below, see eq. (11), that it is realized for strongly cooperative cleavage $\rho_c \ll 1$ or for fast growth at high T-monomer concentrations C_T.

We do not take into account a possible cooperativity in the attachment and detachment process, *i.e.*, ω_{on}, $\omega_{\text{off},T}$, and ω_{off,D^*} do not depend on the state of the last monomer, which is at the tip before attachment or which is left behind at the tip after detachment. We also neglect fracture of filaments, which has been discussed for hemoglobin fibers in ref. [16]. Literature values for cleavage, attachment, and detachment rates of our model are listed in table 1.

We will derive analytic results for the length of the ATP-actin cap, the length distribution of ATP-actin islands, and the cleavage flux. We compare these results to stochastic simulations of the full three-state model, which were performed using the Gillespie algorithm as described in ref. [14]. For sufficiently high T-monomer concentrations C_T, we expect simulation results for the three-state model to agree with our analytic results for the reduced two-state model. In the stochastic simulations, we will use a three-state model with a random $\mathrm{P_i}$ release mechanism with release rate $\omega_r = 0.003\,\mathrm{s}^{-1}$ [3,8]. Furthermore, we use $\omega_{\mathrm{off},\Theta} = 0.2\,\mathrm{s}^{-1}$ [5] and $\omega_{\mathrm{off},D} = 5.4\,\mathrm{s}^{-1}$ [5] for the off-rates of Θ- and D-protomers, respectively.

Growth rate and critical concentrations. – Attachment and detachment parameters for T-monomers lead to the T-protomer growth rate,

$$J_T = \omega_{\mathrm{on}} - P_{1,T}\omega_{\mathrm{off},T} \approx \kappa_{\mathrm{on}} C_T - \omega_{\mathrm{off},T}. \tag{3}$$

Because there is no D*-attachment, $\omega_{\mathrm{on},D^*} = 0$, and we consider the limit $P_{1,D^*} \approx 0$, the T-protomer growth rate J_T equals the total growth rate J_g of the filament,

$$J_g = \omega_{\mathrm{on}} - P_{1,T}\omega_{\mathrm{off},T} - P_{1,D^*}\omega_{\mathrm{off},D^*} \approx J_T. \tag{4}$$

The critical concentration for filament growth at the barbed end is given by $C_{T,g} = \omega_{\mathrm{off},T}/\kappa_{\mathrm{on}}$ with $C_{T,g} \simeq 0.12\,\mu\mathrm{M}$ for the values given in table 1.

For vectorial cleavage with $\rho_c = 0$, there is a single ATP-island at the filament tip and a single TD*-interface, where cleavage takes place with a rate $\omega_{cD^*} = \omega_c$. The length of this ATP-tip becomes infinite in the steady state if the T-protomers growth rate exceeds this cleavage rate, $J_T > \omega_c$, which defines a threshold concentration $C_{T,c} = (\omega_c + \omega_{\mathrm{off},T})/\kappa_{\mathrm{on}}$ with $C_{T,c} \simeq 0.15\,\mu\mathrm{M}$ for the values given in table 1. The dimensionless growth parameter $J_T/\omega_c = (C_T - C_{T,g})/(C_{T,c} - C_{T,g})$ characterizes the competition of growth and hydrolysis currents. Because of condition (2), we will focus on fast growth with $J_T/\omega_c \gg 1$ in the following, see eq. (11) below, which is realized for T-monomer concentrations much larger than the corresponding threshold concentration, $C_T \gg C_{T,c}$.

Length distribution of ATP-tip. – The growing barbed end consists of a sequence of T- and D*-monomers. The state of the filament can be described as a sequence of connected islands of T-monomers which are separated by D*-monomers. Similar to an analysis of the case of random hydrolysis in microtubules in ref. [17] we will focus on the length distribution of these "ATP-islands". First we will consider the length of the *first* ATP-island at the barbed end, which we call "ATP-tip" in the following.

The probability p_k of finding an ATP-tip of length k $k = 0, 1, 2, \ldots$, with $k = 0$ corresponding to the case of a D*-monomer right at the barbed end, satisfies the master equation

$$\begin{aligned}\partial_t p_k = {} & J_T(p_{k-1} - p_k) - \omega_c[1 + \rho_c(k-1)]p_k(1 - \delta_{k,0}) \\ & + \omega_c p_{k+1} + \omega_c \rho_c \sum_{s \geqslant k+2} p_s \end{aligned} \tag{5}$$

with boundary condition $p_{-1} \equiv 0$. The first term on the rhs of eq. (5) describes loss and gain by attachment of T-protomers. The second term is nonzero only for tip lengths $k > 0$ and describes loss by cleavage: the last T-monomer at the TD*-interface is cleaved with a rate ω_{cD^*}, whereas the remaining $k - 1$ T-monomers of the tip are cleaved with a rate ω_{cT}. The last two terms are the corresponding gain terms from cleavage: an ATP-tip length of k can be obtained by cleavage at the TD*-interface of an ATP-tip of length $k + 1$ with rate ω_{cD^*}, or it can be obtained by "fragmentation" of a tip of length $s \geqslant k + 2$ into two pieces by cleavage of its interior T-monomers with rate ω_{cT}. For the special case of random cleavage with $\rho_c = 1$ we recover the results of ref. [17]; for vectorial cleavage with $\rho_c = 0$, eq. (5) reduces to a random walk in k-space ($k > 0$) with stepping probability J_T from $k - 1$ to k and ω_c from $k + 1$ to k. With a continuum approximation in the variable k, eq. (5) has been obtained also in ref. [11].

The steady state of the ATP-tip length distribution p_k is obtained by setting the rhs of eq. (5) equal to zero. It is convenient to consider the cumulative quantity $P_k \equiv \sum_{l \geqslant k} p_l$ with $P_0 = 1$ and $P_1 = P_{1,T}$, for which we find the recursion relation

$$P_{k+1} - P_k = \frac{J_T}{\omega_c(1 - \rho_c)}(P_k - P_{k-1}) + \frac{\rho_c}{1 - \rho_c} k P_k \tag{6}$$

in the steady state with $k \geqslant 1$. For vectorial cleavage with $\rho_c = 0$, we find an exponentially decaying stationary solution $p_k \sim (J_T/\omega_c)^k$ for $J_T < \omega_c$, *i.e.*, below the threshold concentration $C_T < C_{T,c}$. For $J_T > \omega_c$, the ATP-tip is steadily growing and no stationary solution can be found.

For the general case of arbitrary cooperativity, we apply a continuum approximation in the variable k,

$$\begin{gathered} 0 = \partial_k^2 P_k(k) + a\partial_k P_k(k) - bkP_k \quad \text{with} \\ a \equiv 2\frac{1 - \rho_c - J_T/\omega_c}{1 - \rho_c + J_T/\omega_c} \quad \text{and} \quad b \equiv 2\rho_c \frac{1}{1 - \rho_c + J_T/\omega_c}. \end{gathered} \tag{7}$$

The solution of this equation with boundary condition $P_0 = 1$ is

$$P_k = \exp(-ak/2)\frac{\mathrm{Ai}(b^{-2/3}a^2/4 + b^{1/3}k)}{\mathrm{Ai}(b^{-2/3}a^2/4)} \tag{8}$$

where $\mathrm{Ai}(x)$ is the Airy function [18]. The ATP-tip length distribution is obtained as $p_k = P_k - P_{k+1}$ from the solution (8), see fig. 2. The continuum approximation used to derive eq. (7) is justified because neither $|a|$ nor b can become large compared to unity.

In the following we will focus again on fast growth with $J_T/\omega_c \gg 1$, which leads to $a \approx -2$ and $b \approx 2\rho_c\omega_c/J_T \ll 1$. Using the asymptotics of the Airy function, $\mathrm{Ai}(x) \sim e^{-2x^{3/2}/3}$ for $x \gg 1$ [18], we find $P_k \approx e^{-bk^2/2|a|}$ and, consequently, the resulting tip length distribution $p_k \approx -\partial_k P_k(k)$ is exponentially decaying for large k,

$$p_k \approx (kb/|a|)e^{-bk^2/2|a|} \approx k(\omega_c\rho_c/J_T)e^{-k^2\omega_c\rho_c/2J_T}. \tag{9}$$

An interesting observable, which may be experimentally accessible in experiments on single filaments, is the mean

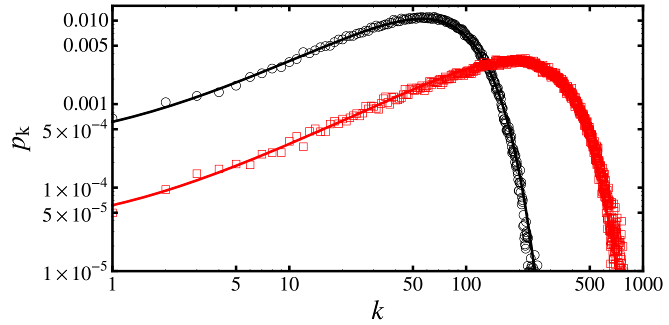

Fig. 2: (Colour on-line) Length distribution p_k of ATP-tip for an actin concentration $C_T = 1\,\mu$M (corresponding to $J_T/\omega_c = 34$) and cleavage parameters $\rho_c = 10^{-2}$ (black, ○) and 10^{-3} (red, □). Other parameter values as in table 1. Comparison between i) analytic results from eq. (8) using $p_k = P_k - P_{k+1}$ (solid lines) and ii) results from stochastic simulations using the Gillespie algorithm (circles).

tip size $\langle k\rangle = \sum_{k\geqslant 1} kp_k$. For fast growth we obtain from eq. (9) a characteristic square-root dependence on the cleavage parameter ρ_c,

$$\langle k\rangle \approx \sqrt{\pi/2}(|a|/b)^{1/2} \approx \sqrt{\pi/2}(J_T/\omega_c\rho_c)^{1/2}, \qquad (10)$$

which could be used in experiments to determine ρ_c by measuring the tip length. Another experimentally accessible observable is the probability P_{1,D^*} that the first monomer is in the D*-state, for which we find

$$P_{1,D^*} = 1 - P_1 \approx \rho_c\omega_c/2J_T, \qquad (11)$$

i.e., a linear dependence on ρ_c. Equation (11) also confirms that the limit $P_{1,D^*} \approx 0$, see (2), is attained for strongly cooperative cleavage $\rho_c \ll 1$ or for fast growth $J_T \gg \omega_c$.

Size distribution of ATP-islands. – Experiments probing the structure of single filaments can give information not only on the length of the ATP-tip but the whole distribution of ATP-islands sizes in the filament. The average number I_k of ATP-islands of length k fulfills the master equation

$$\begin{aligned}\partial_t I_k \;=\;& J_T(p_{k-1} - p_k) - \omega_c(1 + (k-1)\rho_c)I_k\\ &+ \omega_c(1+\rho_c)I_{k+1} + 2\omega_c\rho_c \sum_{s\geqslant k+2} I_s \end{aligned}\qquad (12)$$

for $k \geqslant 1$. The first term on the rhs of eq. (12) gives the change in ATP-island numbers from attachment and detachment at the tip. The second term describes the loss from cleavage at the $k-1$ sites of the ATP-island with T-neighbors on the pointed side with rate ω_{cT} and the loss from cleavage with rate ω_{cD^*} at the TD*-interface at the pointed side of the island. The third and fourth terms on the rhs of eq. (12) are gain terms from cleavage at an interior site of an island. The fourth term means that any ATP-island of length k can be obtained by "fragmentation" of an island of length $s \geqslant k+2$ in two ways with a rate ω_{cT} for each way. The third term means that an ATP-island of length k can also be obtained by cleavage at the boundaries of an ATP-island of length $k+1$ with rate ω_{cT} on the barbed side and with rate ω_{cD^*} on the pointed side of the island.

Two important quantities, which follow from the ATP-island distribution and can be observed in experiments on single actin filaments, are the average total number of ATP-islands $I \equiv \sum_{k\geqslant 1} I_k$ and the average total number of ATP-actin protomers $\langle N_T\rangle \equiv \sum_{k\geqslant 1} kI_k$. The average total number $\langle N_T\rangle$ of ATP-actin protomers gives a measure of the average total length of the ATP-cap of the actin filament. The average total number of ATP-islands I also gives the number of TD*-interfaces within the ATP-cap, where cleavage takes place with rate ω_{cD^*}. Knowledge of these two quantities therefore not only characterizes the filament structure but allows us to also calculate the resulting cleavage flux. For the two quantities I and $\langle N_T\rangle$, we obtain the rate equations

$$\partial_t I = J_T p_0 + \omega_c\rho_c(\langle N_T\rangle - 2I) - \omega_c(1-\rho_c)I_1, \qquad (13)$$

$$\partial_t\langle N_T\rangle = J_T - \omega_c\rho_c(\langle N_T\rangle - I) - \omega_c I. \qquad (14)$$

Equation (13) describes the creation of additional ATP-islands by addition of T-monomers at an empty tip or by cleavage in the interior of an existing T-island with rate ω_{cT}, whereas the island number is reduced by cleavage of ATP-islands of unit length with a rate ω_{cD^*}. The first term on the rhs of eq. (14) describes the addition of T-monomers with the rate J_T, the last two terms the loss of T-protomers by cleavage: the total number of TD*-interfaces with a cleavage rate ω_{cD^*} is given by I, whereas the number of sites where cleavage happens with the slower rate ω_{cT} is given by $\langle N_T\rangle - I$. Therefore, the total cleavage flux is given by

$$J_c = \omega_c\rho_c(\langle N_T\rangle - I) + \omega_c I \qquad (15)$$

and eq. (14) is equivalent to $\partial_t\langle N_T\rangle = J_T - J_c$: In a steady state we must have $J_T = J_c$, *i.e.*, T-protomer addition flux and cleavage flux balance.

The steady state of the ATP-island distribution I_k fulfills $\partial_t I_k = 0$. We determine the stationary island distribution for fast growth in two steps: i) We obtain a differential equation for I_k in k by requiring that $\partial_t(I_k - I_{k-1}) = 0$. This will give the stationary I_k apart from one integration constant. ii) We will determine this integration constant by looking for stationary solutions of eq. (14) for $\langle N_T\rangle$.

i) To determine the steady-state ATP-island distribution from eq. (12), we consider $\partial_t(I_k - I_{k-1})$ for $k \geqslant 2$ and use continuous k, which leads to

$$\begin{aligned}\partial_t(I_k - I_{k-1}) \;\approx\;& -J_T\partial_k^2 p_k(k-1) + (\omega_c - \omega_c\rho_c)\,\partial_k^2 I_k(k)\\ &-\omega_c\rho_c(k-1)\partial_k I_k(k) - 3\omega_c\rho_c I_k. \end{aligned}\qquad (16)$$

The steady state fulfills $\partial_t(I_k - I_{k-1}) = 0$. In the limit of fast growth, the term $J_T\partial_k^2 p_k$ is exponentially small, and we find

$$I_k = c_I \mathcal{I}\left(\sqrt{2\rho_c}(k-1)\right). \tag{17}$$

The integration constant c_I has yet to be determined. The scaling function $\mathcal{I}(x) = 2^{-3/2}D_{-3}(x/\sqrt{2})e^{x^2/8}$, where $D_\nu(x)$ is Whittaker's parabolic cylinder function [18], fulfills the differential equation

$$0 = 2\mathcal{I}''(x) - x\mathcal{I}'(x) - 3\mathcal{I}(x). \tag{18}$$

It decays as $\mathcal{I}(x) \approx x^{-3}$ for $x \gg 1$, which gives rise to a power-law tail in the island distribution with the same scaling behavior $I_k \sim k^{-3}$ as for random cleavage [17]. From the island distribution (17), we derive

$$\begin{aligned} I &\approx \frac{c_I}{\sqrt{2\rho_c}}\int_0^\infty \mathrm{d}x\mathcal{I}(x) = \frac{c_I}{4\sqrt{2\rho_c}}, \\ \langle N_T\rangle &\approx \frac{c_I}{2\rho_c}\int_0^\infty \mathrm{d}x x\mathcal{I}(x) = \frac{\sqrt{\pi}c_I}{8\rho_c}, \end{aligned} \tag{19}$$

where we used the relations $\int_0^\infty \mathrm{d}x\mathcal{I}(x) = -\mathcal{I}'(0) = 1/4$ and $\int_0^\infty \mathrm{d}x x\mathcal{I}(x) = 2\mathcal{I}(0) = \sqrt{\pi}/4$, which follow from the differential equation (18).

ii) Using the results (19) in eq. (14) and requiring stationarity $\partial_t\langle N_T\rangle = 0$ to leading order in ρ_c, we determine the integration constant

$$c_I \approx 4\sqrt{2}J_T\sqrt{\rho_c}/\omega_c. \tag{20}$$

This leads to the final results

$$I_1 \approx \sqrt{\frac{\pi}{2}}\frac{J_T\sqrt{\rho_c}}{\omega_c}, \quad I \approx \frac{J_T}{\omega_c}, \quad \langle N_T\rangle \approx \sqrt{\frac{\pi}{2}}\frac{J_T}{\omega_c\sqrt{\rho_c}}. \tag{21}$$

for the average total length $\langle N_T\rangle$ of the ATP-cap, the total number of ATP-islands I and the number I_1 of short ATP-islands of unit length, see fig. 3. The result $I \approx J_T/\omega_c \gg 1$ for the total number of ATP-islands is remarkable because we have $I = 1$ for strictly vectorial cleavage. Thus a small cleavage parameter $\rho_c \neq 0$ constitutes a singular perturbation, which gives rise to a pronounced change in the ATP-cap structure with a dramatic increase in the total number of ATP-islands.

ATP-cap length and cleavage flux. – The scaling behavior of I_k in eq. (21) leads to a characteristic scaling of island sizes k with the square root of the cleavage parameter ρ_c, which determines the ρ_c-dependence of experimental observables such as the average total length of the ATP-cap length $\langle N_T\rangle$ and the cleavage flux J_c.

According to (21) the ATP-cap length $\langle N_T\rangle$ depends linearly on the T-protomer growth rate J_T and, thus, on the concentration C_T of T-monomers and increases $\propto 1/\sqrt{\rho_c}$ for small cleavage parameters corresponding to strongly cooperative cleavage mechanisms, see fig. 4(a). This result is corroborated by a scaling argument [14].

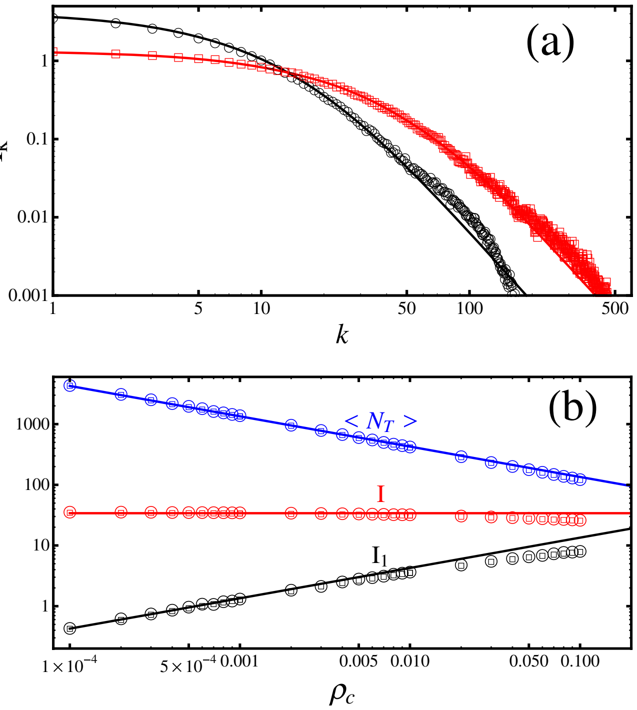

Fig. 3: (Colour on-line) (a) Double-logarithmic plot of the size distribution I_k of ATP-islands for an actin concentration $C_T = 1\,\mu$M (corresponding to $J_T/\omega_c = 34$) and cleavage parameters $\rho_c = 10^{-2}$ (black, ○) and 10^{-3} (red, □). Other parameter values are as in table 1. Comparison between i) analytic results from eq. (21) (solid lines) and ii) results from stochastic simulations using the Gillespie algorithm (circles). (b) Double-logarithmic plot of $\langle N_T\rangle$ (blue), I (red), and I_1 (black) in the steady state as a function of ρ_c for $C_T = 1\,\mu$M ($J_T/\omega_c = 34$). Comparison between i) analytic results from eq. (21) (solid lines), ii) results from a stochastic simulations using the Gillespie algorithm (circles), and iii) results from a numerical integration of the full master equations (5) and (12) (squares).

It shows that experiments on the total cap length in the limit of fast growth will allow to determine the cleavage parameter ρ_c if the cleavage rate is known. On the other hand, the cap length in (21) only depends on the *product* $1/\omega_c\sqrt{\rho_c} = 1/\sqrt{\omega_{c,D^*}\omega_{c,T}}$. Thus, a mechanism with high cooperativity and large cleavage rate can give rise to a similar cap length as a random cleavage process with a low cleavage rate. This demonstrates that measurements of certain filament properties such as the ATP monomer content of filaments do not allow to uniquely distinguish between a vectorial model with high cleavage rate [6–9] and a random model with lower cleavage rate [3–5].

From the coupled rate eqs. (13) and (14) for I and $\langle N_T\rangle$, we can also calculate the characteristic time scale $\tau \approx 1/\omega_c\sqrt{\rho_c}$ for relaxation to the steady state with stationary values (21). This experimentally relevant time scale is increasing with the same $\rho_c^{-1/2}$-dependence as the steady-state ATP-cap length for small cleavage parameters.

According to eqs. (14) and (15), the cleavage flux J_c and the T-protomer addition flux J_T must balance in

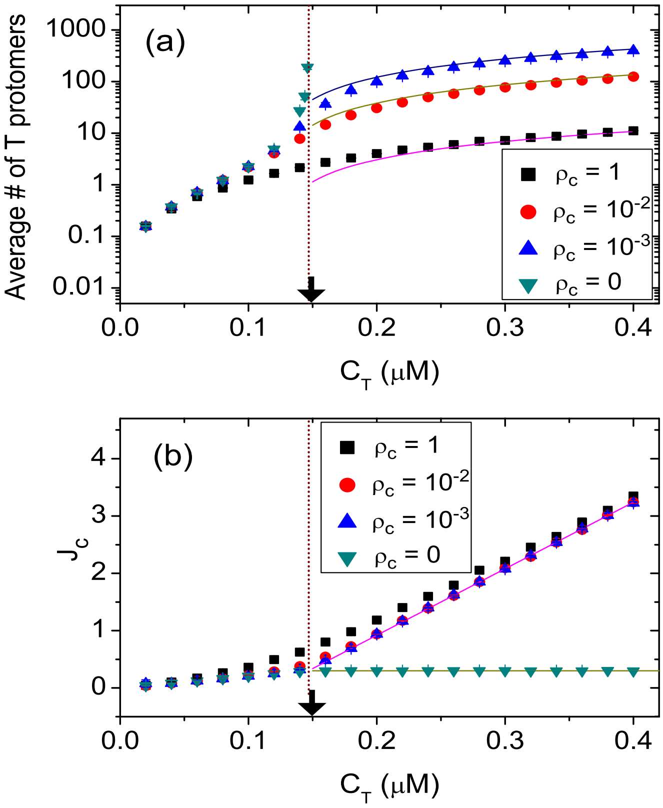

Fig. 4: (Colour on-line) (a) The total average ATP-cap length $\langle N_T \rangle$ and (b) the total cleavage flux J_c as a function of actin concentration C_T for different cleavage parameters ρ_c. Comparison between i) analytic results for $C_T \gg C_{T,c}$ (the critical concentration $C_{T,c}$ is marked by an arrow) in the regime of fast growth (solid lines) and ii) results from a stochastic simulations using the Gillespie algorithm (data points).

the steady state, *i.e.*, $J_c = J_T$. Because of eq. (3) the cleavage flux depends then *linearly* on the T-monomer concentration C_T and becomes *independent* of the cooperativity parameter for fast growth with $P_{1,T} \approx 1$, see fig. 4(b). For vectorial cleavage, on the other hand, we have $I = 1$, and the cleavage flux is directly given by the cleavage rate, $J_c = \omega_c$ and, thus, *independent* of the T-monomer concentration, see fig. 4(b). This shows again that a non-zero cleavage parameter represents a singular perturbation of vectorial cleavage, and the cleavage flux is a sensitive quantity to differentiate between strictly vectorial cleavage with $\rho_c = 0$ and strongly cooperative cleavage with small but nonzero ρ_c.

Conclusion. – In conclusion, we have introduced an effective two-state model for cooperative ATP-hydrolysis in actin filaments, where cooperativity is characterized by the cleavage parameter ρ_c. The model contains random ($\rho_c = 1$) and vectorial ($\rho_c = 0$) cleavage as special cases. For this two-state model, we could obtain analytic steady-state results for quantities such as the size of the ATP-actin cap, the size distribution of ATP-actin islands, the total number of ATP-actin islands, which describe the structure of the actin filament, and kinetic quantities such as the cleavage flux. Measurements of these steady-state quantities will allow to determine the cleavage rate and the cooperativity of the ATP-cleavage mechanism. Recently depolymerization experiments on individual actin filaments have become possible [5,19], which allow to obtain information on filament structure based on the different depolymerization rates of T-, Θ- and D-monomers.

The depolymerization experiments in ref. [19] as analyzed in ref. [14] and earlier kinetic data discussed in refs. [7,10] suggest that the cleavage parameter ρ_c is as small as 10^{-5}–10^{-6} and that cleavage is thus strongly cooperative. Our analytic results become exact in the limit of small ρ_c and fast growth $J_T \gg \omega_c$ and, thus, can be directly applied in this relevant parameter regime. Measurements of force-velocity relations for polymerization under force can also provide sensitive probes of the filament structure as discussed in ref. [20].

REFERENCES

[1] Bray D., *Cell Movements: From Molecules to Motility*, Vol. **2** (Garland Publishing) 2001.
[2] Theriot J. A., *Traffic*, **19** (2000) 1.
[3] Blanchoin L. and Pollard T. D., *Biochemistry*, **41** (2002) 597.
[4] Vavylonis D., Yang Q. and O'Shaughnessy B., *Proc. Natl. Acad. Sci. U.S.A.*, **100** (2005) 8543.
[5] Fujiwara I., Vavylonis D. and Pollard T. D., *Proc. Natl. Acad. Sci. U.S.A.*, **104** (2007) 8827.
[6] Pantaloni D., Hill T. L., Carlier M.-F. and Korn E. D., *Proc. Natl. Acad. Sci. U.S.A.*, **82** (1985) 7207.
[7] Korn E. D., Carlier M.-F. and Pantaloni D., *Science*, **238** (1987) 638.
[8] Melki R., Fievez S. and Carlier M.-F., *Biochemistry*, **35** (1996) 12038.
[9] Stukalin E. B. and Kolomeisky A. B., *Biophys. J.*, **90** (2006) 2673.
[10] Carlier M.-F., Pantaloni D. and Korn E., *J. Biol. Chem.*, **262** (1987) 3052.
[11] Flyvbjerg H., Holy T. E. and Leibler S., *Phys. Rev. Lett.*, **73** (1994) 2372.
[12] Graceffa P. and Dominguez R., *J. Biol. Chem.*, **278** (2003) 34172.
[13] Rould M. A., Wan Q., Joel P. B., Lowey S. and Trybus K. M., *J. Biol. Chem.*, **281** (2006) 31909.
[14] Li X., Kierfeld J. and Lipowsky R., *Phys. Rev. Lett.*, **103** (2009) 148102.
[15] Pollard T. D., *J. Cell Biol.*, **103** (1986) 2747.
[16] Wang J. C., Kwong S., Ferrone F. A., Turner M. S. and Briehl R. W., *Biophys. J.*, **96** (2009) 655.
[17] Antal T., Krapivsky P. L., Redner S., Mailman M. and Chakraborty B., *Phys. Rev. E*, **76** (2007) 041907.
[18] Abramowitz M., *Pocketbook of Mathematical Functions* (Deutsch, Thun) 1984.
[19] Kueh H. Y., Brieher W. M. and Mitchison T. J., *Proc. Natl. Acad. Sci. U.S.A.*, **105** (2008) 16531.
[20] Ranjith P., Lacoste D., Mallick K. and Joanny J.-F., *Biophys. J.*, **96** (2009) 2146.